

Creation of Brønsted acid sites on Sn-based solid catalysts for the conversion of biomass†

Cite this: *J. Mater. Chem. A*, 2014, 2, 3725Received 2nd December 2013
Accepted 19th December 2013

DOI: 10.1039/c3ta14982j

www.rsc.org/MaterialsA

Liang Wang,^a Jian Zhang,^a Xuefeng Wang,^{bg} Bingsen Zhang,^d Weijie Ji,^e
Xiangju Meng,^a Jixue Li,^f Dang Sheng Su,^{*cd} Xinhe Bao^{*b} and Feng-Shou Xiao^{*a}

Hydroxyl-attached Sn species are highly dispersed on the surface of mesoporous silica (SBA-15) by the grafting of dimethyldichlorostannane followed by calcination to transform the methyl groups into hydroxyl groups (S–Sn–OH). S–Sn–OH has both Lewis and Brønsted acidic sites, resulting in superior catalytic activities in the acetalisation of glycerol.

Brønsted acid catalysts are of great significance in chemical research and industrial processes.^{1–3} Notably, homogeneous Brønsted acid catalysts such as H₂SO₄ and HCl are widely used,³ but they are difficult to separate and regenerate from the reaction systems, making these processes costly and environmentally unfriendly. Compared with homogeneous Brønsted acid catalysts, heterogeneous systems are preferred because of their inherent advantages of easy separation and recyclability.^{4–6} However, the synthesis of highly active and stable heterogeneous Brønsted acid catalysts is still a challenge.

Currently, the introduction of metal atoms into the solid supports is regarded as a typical method to generate heterogeneous acids. One of the most well-known cases is the introduction of Al atoms into silica, producing Brønsted acid sites.^{6,7} For example, microporous aluminosilicate zeolites, which

contain highly dispersed Al atoms in the silica framework, are typical Brønsted acid catalysts and have been widely used in many industrial processes. However, the small pores of zeolites strongly limit their use in the conversion of bulky molecules.⁶ Therefore, great efforts have been devoted to synthesizing mesoporous aluminosilicates,⁷ but their weak acidity severely hinders their wide application due to the amorphous nature of the mesoporous walls. This phenomenon is due to the fact that the Brønsted acid sites of aluminosilicate originate from the protons which are present to neutralize the negative charges of the aluminosilicate walls (Scheme S1a†). Besides Al atoms, introducing Sn atoms into mesoporous silica would also generate efficient solid acids, but their acidic sites are only Lewis type (Scheme S1b†), which cannot catalyze reactions requiring Brønsted acid sites.⁸ Therefore, it is a challenge to develop alternative Sn-based catalysts with Brønsted acid sites.

In this work, we propose a simple strategy to create Brønsted acid site on Sn-decorated mesoporous materials. By calcination of dimethyl-modified Sn on the surface of SBA-15 mesoporous silica (S–Sn–Me), a hydroxyl-attached Sn species (S–Sn–OH) is created (Fig. 1a), which has Brønsted acid properties. Very interestingly, catalytic tests in a model reaction of biomass conversion, *i.e.*, acetalisation of glycerol with acetone to form solketal (2,2-dimethyl-1,3-dioxolane-4-methanol) show that the S–Sn–OH catalyst is very active, compared with conventional Sn-based catalysts.

The S–Sn–OH sample with a Si : Sn molar ratio of 66 was synthesized by the grafting of dimethyldichlorostannane onto SBA-15, followed by calcination at 600 °C for 3 h. Fig. S1A† shows the small-angle XRD patterns of the SBA-15, S–Sn–Me, and S–Sn–OH samples. In the region 0.6–2°, all three samples show three well-resolved peaks that could be indexed to the (110), (200), and (211) reflections of hexagonal mesoporous arrays (Fig. S1A†), indicating that the hexagonal mesostructure remains stable during the synthesis of S–Sn–OH.⁹ The nitrogen sorption isotherms of S–Sn–OH exhibit a typical type-IV curve, with a hysteresis loop at relative pressure of 0.54–0.79 (Fig. S1B†), indicating the typical mesoporous structure of

^aKey Lab of Applied Chemistry of Zhejiang Province, Zhejiang University, Hangzhou 310028, China. E-mail: fsxiao@zju.edu.cn

^bState Key Laboratory for Catalysis, Dalian Institute of Chemical Physics, Chinese Academy of Science, Dalian 116023, China. E-mail: xhbao@dicp.ac.cn

^cDepartment of Inorganic Chemistry, Fritz Haber Institute of the Max Planck Society, Berlin 14195, Germany. E-mail: dangsheng@fhi-berlin.mpg.de

^dShenyang National Laboratory of Materials Science Institute of Metal Research, Chinese Academy of Science, Shenyang 110016, China

^eKey Laboratory of Mesoscopic Chemistry, MOE, Department of Chemistry, Nanjing University, Nanjing 210093, China

^fDepartment of Materials Science and Engineering, Zhejiang University, Hangzhou 310028, China

^gSchool of Environment and Chemical Engineering, Dalian University, Dalian 116622, China

† Electronic supplementary information (ESI) available. See DOI: 10.1039/c3ta14982j

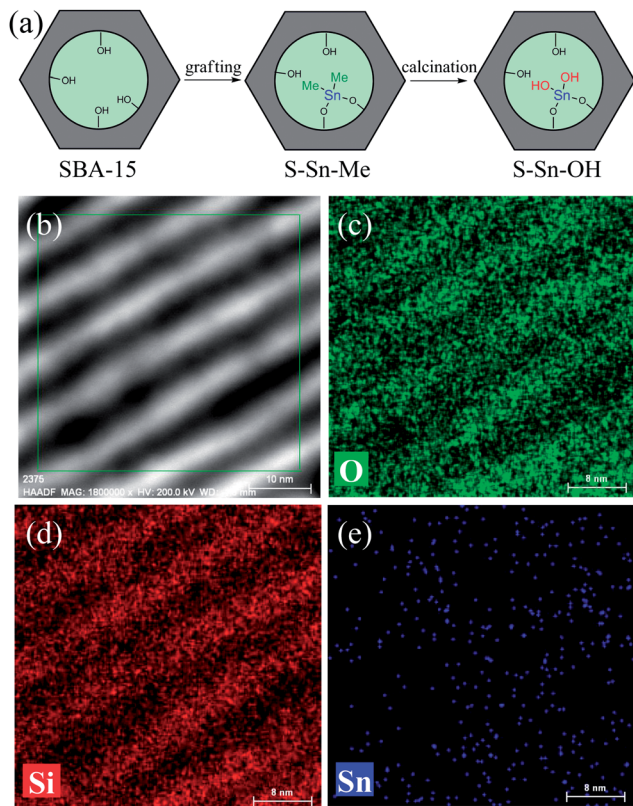


Fig. 1 (a) Scheme for the synthesis of S-Sn-OH; (b) STEM image, and (c) O, (d) Si, and (e) Sn EDS elemental maps of S-Sn-OH. The scale bars in the images are 10, 8, 8, and 8 nm, respectively.

S-Sn-OH¹⁰ which could also be directly observed from the TEM images (Fig. S2†). The S-Sn-Me and S-Sn-OH samples have relatively low surface areas of 635–677 m² g⁻¹ and a pore size distribution of 7.5 nm compared with the as-synthesized SBA-15 (930 m² g⁻¹ and 8.2 nm, Table S1†). This phenomenon might be due to the presence of Sn species in the mesopores of SBA-15.¹¹

Fig. S3† presents the energy dispersive X-ray (EDX) analyses of S-Sn-OH, which show obvious signals associated with Sn species. It is also worth noting that the Si : Sn ratios are very similar in the randomly selected areas in S-Sn-OH. Interestingly, peaks associated with metallic Sn or SnO₂ crystals were undetectable in the wide angle XRD pattern of S-Sn-OH (Fig. S4†), and Sn species could not be directly observed even in the high-resolution STEM images (Fig. 1b and S5a†). These results suggest the extremely high dispersion of Sn species on the surface of mesoporous silica. Furthermore, we performed elemental mapping analysis of S-Sn-OH (Fig. 1b–e and S5†), from which highly dispersed Sn was directly observed in different areas of S-Sn-OH (Fig. 1e and S5d†).

Fig. 2A shows the Sn 3d XPS spectra of S-Sn-Me and S-Sn-OH, with the Sn 3d_{5/2} peak at 487.7 eV, which is obviously higher than that of the SnO₂ crystals (485.8 eV). This phenomenon can reasonably be attributed to the high dispersion of Sn species.¹² Fig. 2B shows UV-visible spectra of the various Sn-based samples. The conventional Sn-SBA-15 shows a band at 220 nm, associated with typical Sn(OSi)₄ species (Fig. 2B-c). However, S-Sn-Me and S-Sn-OH show bands at 250–255 nm

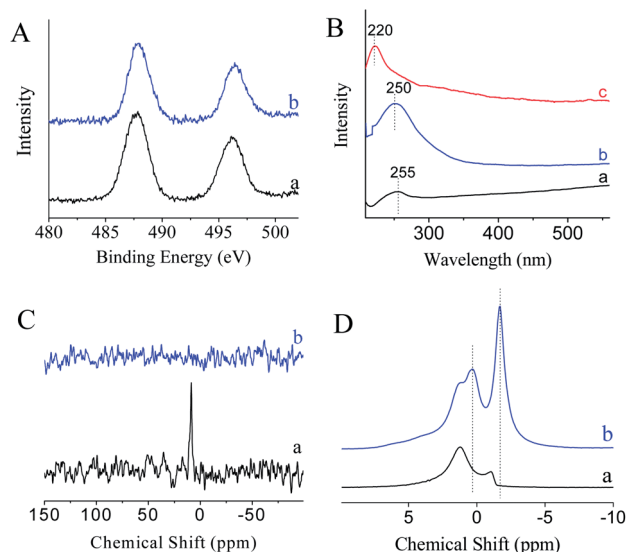


Fig. 2 (A) Sn 3d XPS, (B) UV-visible, (C) ¹³C NMR, and (D) ¹H NMR spectra of (a) S-Sn-Me, (b) S-Sn-OH, and (c) Sn-SBA-15.

(Fig. 2B-a and b). This phenomenon might be due to the presence of –Me or –OH groups on the Sn species, leading to a change in the electron charge transfer for Sn species.¹³ Fig. 2C shows ¹³C spectra of S-Sn-Me and S-Sn-OH. As we expected, S-Sn-Me exhibits an obvious signal at 8.3 ppm, which could be assigned to –Me groups attached to Sn species (Fig. 2C-a). In contrast, the signal at 8.3 ppm is absent in the spectrum of S-Sn-OH (Fig. 2C-b), indicating the dispersion of the –Me groups after the calcination. Fig. 2D shows ¹H NMR spectra of S-Sn-Me and S-Sn-OH. Compared with S-Sn-Me, S-Sn-OH shows additional signals at 0.3 and –1.7 ppm, which could reasonably be assigned to the contribution from Sn–OH groups, because the only difference between S-Sn-Me and S-Sn-OH is the transformation of the –Me groups on the Sn species to –OH groups.

Fig. 3 shows the IR spectra of pyridine adsorption on the S-Sn-Me and S-Sn-OH samples. The bands at 1454 and 1615 cm⁻¹, which are assigned to coordinatively bound pyridine

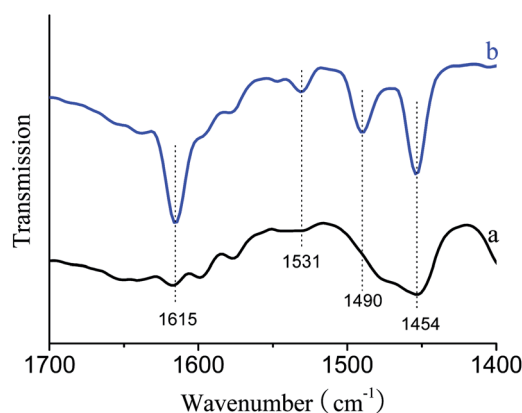


Fig. 3 Pyridine adsorption IR spectra of (a) S-Sn-Me and (b) S-Sn-OH.

on Lewis acid sites,¹⁴ exist in both S-Sn-Me and S-Sn-OH. Compared with S-Sn-Me, the spectrum of S-Sn-OH shows an additional band at 1531 cm⁻¹, which is characteristic of pyridine adsorbed on Brønsted acid sites.^{14a,15} These results indicate that S-Sn-Me contains only Lewis acid sites, while S-Sn-OH has both Lewis and Brønsted acid sites. Notably, the acidity of S-Sn-OH is strongly dependent on the synthesis conditions. For example, increasing the Sn content by changing the Si : Sn ratio from 66 to 35, results in the formation of a Sn-based sample (S-Sn-C1). In the pyridine adsorption IR spectrum, the S-Sn-C1 sample shows three bands at 1453, 1490, and 1613 cm⁻¹, associated with characteristic vibrations of pyridine adsorbed on Lewis acids (Fig. S6a and Table S1†). Fig. S7† shows the XRD pattern of S-Sn-C1, with obvious peaks at 34.1 and 51.9°, associated with the (101) and (210) planes of SnO₂ crystals. Fig. S8† shows the STEM image and Sn EDS elemental map of S-Sn-C1, which provide direct observation of the SnO₂ crystals. These results suggest that the aggregation of highly dispersed Sn species (*e.g.* S-Sn-OH) into bulk SnO₂ crystals (*e.g.* S-Sn-C1) would lead to the dispersion of Brønsted acid sites, which might be due to the loss of most of the Sn-OH groups on the bulk SnO₂ crystals. Additionally, when the S-Sn-Me sample was calcined at 800 °C (S-Sn-C2), no bands associated with adsorbed pyridine were observed in the pyridine adsorption IR spectrum (Fig. S6b†). The Si : Sn ratio in S-Sn-C2 was established to be higher than 200 (Table S1†), indicating the loss of Sn species during the calcination at 800 °C. This phenomenon might be due to the fact that the SBA-15 support and the highly dispersed Sn species are unstable at relatively high temperatures (800 °C).

Glycerol, a major by-product in the production of biodiesel, is produced in large amounts every year. Recently, the conversion of glycerol to more valuable products has been a hot topic. Here, the acetalisation of glycerol with acetone (Fig. 4A) was employed as a model reaction because of the high value of the solketal product.¹⁶ Both Lewis and Brønsted acid sites are active for the acetalisation of glycerol with acetone, but the Brønsted acids are reported to be more active than Lewis ones.¹⁷ Fig. 4B shows the catalytic data over various acid catalysts; solketal selectivity is higher than 98% in most cases. S-Sn-Me and conventional Sn-SBA-15 catalysts, which are typical Lewis acids,¹⁸ show glycerol conversions of 26.9 and 42.2%, respectively. Interestingly, S-Sn-OH, with both Lewis and Brønsted acid sites, exhibits a glycerol conversion as high as 84.1%, which is very similar to that (83.0%) of the homogeneous H₂SO₄ catalyst. Notably, S-Sn-OH gives a productivity of solketal of 663.7 mol h⁻¹ mol_{Sn}⁻¹ (Fig. S9†), which is much higher than those over Sn-SBA-15 (249.0 mol h⁻¹ mol_{Sn}⁻¹), S-Sn-Me (213.0 mol h⁻¹ mol_{Sn}⁻¹), and Al-SBA-15 (59.0 mol h⁻¹ mol_{Al}⁻¹). These results indicate the superior catalytic activity of S-Sn-OH in the acetalisation of glycerol. Considering that the difference between S-Sn-Me and S-Sn-OH is only the presence of Brønsted acid sites, the higher activity of S-Sn-OH than that of S-Sn-Me should be attributed to the contribution of Brønsted acids. The H-ZSM-5, H-USY, and Al-SBA-15 catalysts, which are reported acid catalysts with both Lewis and Brønsted sites,¹⁹ exhibit glycerol conversions of 24.0, 39.2%, and 65.0%, respectively. These results are all lower than that of S-Sn-OH (84.1%), which might be because that the small

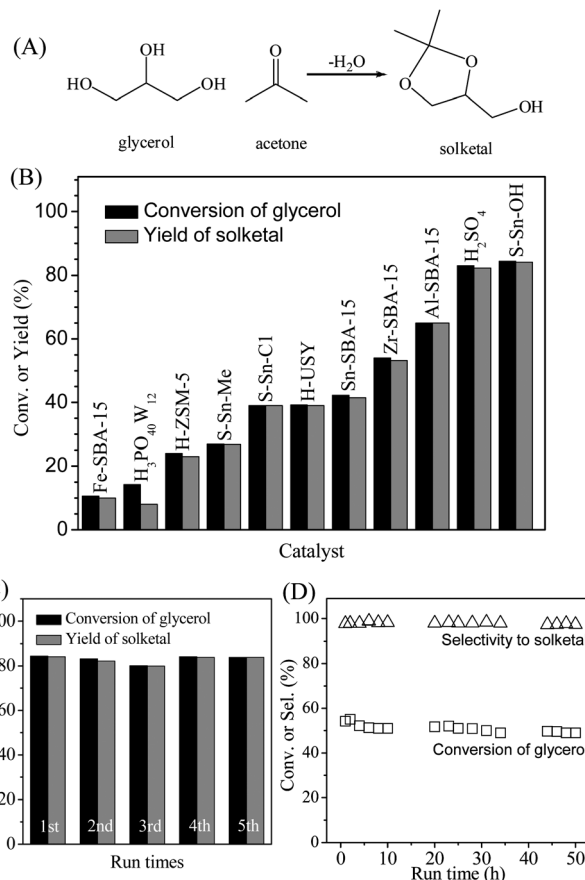


Fig. 4 (A) Scheme for the acetalisation of glycerol with acetone to produce solketal; (B) catalytic data over various catalysts. Reaction conditions: 10 mmol of glycerol, 10 mmol of acetone, 4 g of *t*-BuOH, and 50 mg of solid catalyst or 6 mg of H₂SO₄, with the temperature of the oil bath at 80 °C for 6 h; (C) recycling test of S-Sn-Me: the sample was treated in air at 400 °C for 2 h after the 3rd use; (D) the acetalisation of glycerol over S-Sn-Me in a fixed-bed reactor. Reaction conditions: 0.1 g of S-Sn-OH catalyst, glycerol and acetone in *t*-BuOH solution (16.7 wt% of glycerol, molar ratio of glycerol : acetone = 1 : 1), 80 °C, 0.2 ml min⁻¹.

pore size of H-ZSM-5 does not permit the acetalisation to occur inside the pores; H-USY is an aluminium-rich zeolite with a hydrophilic surface, which could keep the formed water inside the pores, weakening the acid sites and inhibiting the acetalisation; the Al-SBA-15 catalyst has Al species in the amorphous silica walls, leading to weak acidity.^{17b,c}

Fig. 4C shows the recyclability test of the S-Sn-OH catalyst. Even after 4 cycles, S-Sn-OH still gives a high conversion of glycerol of 83.8%. Additionally, after separating the solid catalyst from the reaction system, Sn content in the liquor was undetectable, suggesting there is essentially no leaching of the S-Sn-OH catalyst. More importantly, we tested the catalytic life of S-Sn-OH in a continuous reaction system with a low conversion of glycerol. As shown in Fig. 4D, the glycerol conversion and solketal yield show no obvious decrease in glycerol conversion (49.0–55.2%) and solketal selectivity (97.4–99.0%) over a reaction period of 50 h. These results indicate the high stability and good recyclability of S-Sn-OH for the acetalisation of glycerol with acetone, which offers a good opportunity

for potentially wide applications of the S-Sn-OH catalyst in the future.

The Sn catalysts were also used to catalyze the conversion of fructose in ethanol (Scheme S2 and Table S2†), which could produce different products depending on the nature of the catalyst acidity.^{3a,b,19a,20a} For example, ethyl lactate would be formed as major product over Lewis catalysts (Route 1 in Scheme S2†),²⁰ while HMF could be formed as the major product over Brønsted acids or Brønsted and Lewis acids. Further conversion of HMF leads to the formation of ethoxymethylfurfural and ethyl levulinate (Route 2 in Scheme S2†).^{20,21} Sn-SBA-15, S-Sn-Me, and S-Sn-OH catalysts give high fructose conversion (82.3–100%), but their product selectivities are quite different. Sn-SBA-15 and S-Sn-Me catalysts with Lewis acid sites generate ethyl lactate as the major product (23.9 and 10.2%). However, S-Sn-OH, with both Lewis and Brønsted acid sites, generates major products of ethyl levulinate and ethoxymethylfurfural. These results are explained by the fact that the presence of Brønsted acid sites on S-Sn-OH can effectively catalyze the conversion of fructose through Route 2.

In summary, an alternative Sn catalyst with Brønsted acid sites (S-Sn-OH) was created by grafting hydroxyl-attached Sn species onto the surface of SBA-15. The S-Sn-OH catalyst with Brønsted acid sites shows outstanding performance in the acetalisation of glycerol, a valuable reaction for the utilization of biomass. The results reported here are highly significant since Brønsted acids play important roles in the fields of fuels and energy. The strategy reported in this work will allow the development of more novel Brønsted acid catalysts in the future, which is currently under investigation.

This work was supported by the National Natural Science Foundation of China (21333009, 21273197, U1162201, 21203215), the National High-Tech Research and Development program of China (2013AA065301), the Fundamental Research Funds for the Central Universities (2013XZZX001), financial support provided by the IMR SYNL-T.S. Ke Research Fellowship, and the China Post-doctoral Science Foundation (2012M520652). We thank Prof. L. J. Song and Prof. H. C. Guo for help in IR characterizations.

Notes and references

- (a) P. Barbaro and F. Liguori, *Chem. Rev.*, 2009, **109**, 515; (b) A. Corma, *Chem. Rev.*, 1995, **95**, 559.
- (a) M. E. Davis, *Nature*, 2002, **417**, 813; (b) C. W. Jones, K. Tsuji and M. E. Davis, *Nature*, 1998, **393**, 52; (c) T. K. Cheung and B. C. Gates, *J. Catal.*, 1997, **168**, 522; (d) W. F. Yan, E. W. Hagaman and S. Dai, *Chem. Mater.*, 2004, **16**, 5182; (e) J. A. Melero, G. D. Stucky, R. van Grieken and G. Morales, *J. Mater. Chem.*, 2002, **12**, 1664.
- (a) Y. Roman-Leshkov, J. N. Chheda and J. A. Dumesic, *Science*, 2006, **312**, 1933; (b) J. B. Binder and R. T. Raines, *J. Am. Chem. Soc.*, 2009, **131**, 1979; (c) G. Yong, Y. Zhang and J. Y. Ying, *Angew. Chem., Int. Ed.*, 2008, **47**, 9345.
- (a) A. Corma and H. Garcia, *Chem. Rev.*, 2003, **103**, 4307; (b) M. Hara, T. Yoshida, A. Takagaki, T. Takada, J. N. Kondo, S. Hayashi and K. Domen, *Angew. Chem., Int. Ed.*, 2004, **43**, 2955.
- (a) R. Rinaldi, R. Palkovits and F. Schuth, *Angew. Chem., Int. Ed.*, 2008, **47**, 8047; (b) Y. Wang, F. Wang, Q. Song, Q. Xin, S. Xu and J. Xu, *J. Am. Chem. Soc.*, 2013, **135**, 1506; (c) Y. Lee, M. B. Park, P. S. Kim, A. Vicente, C. Fernandez, I.-S. Nam and S. B. Hong, *ACS Catal.*, 2013, **3**, 617.
- (a) T. Yokoi, M. Yoshioka, H. Imai and T. Tatsumi, *Angew. Chem., Int. Ed.*, 2009, **48**, 9884; (b) F.-S. Xiao, L. F. Wang, C. Y. Yin, K. F. Lin, Y. Di, J. Li, R. Xu, D. S. Su, R. Schlögl, T. Yokoi and T. Tatsumi, *Angew. Chem., Int. Ed.*, 2006, **45**, 3090; (c) F. Liu, T. Willhammar, L. Wang, L. Zhu, Q. Sun, X. Meng, W. Carrillo-Cabrera, X. Zou and F.-S. Xiao, *J. Am. Chem. Soc.*, 2012, **134**, 4557; (d) X. Y. Yang, G. Tian, L. H. Chen, Y. Li, J. C. Rooke, Y.-X. Wei, Z.-M. Liu, D. Zhao, G. Van Tendeloo and B.-L. Su, *Chem.-Eur. J.*, 2011, **17**, 14987; (e) J. C. Kang, K. Cheng, L. Zhang, Q. Zhang, J. Ding, W. Hua, Y. Lou, Q. Zhai and Y. Wang, *Angew. Chem., Int. Ed.*, 2011, **50**, 5200; (f) J. Zhou, Z. Hua, Z. Liu, W. Wu, Y. Zhu and J. L. Shi, *ACS Catal.*, 2011, **1**, 287; (g) X. Zhang, D. Liu, D. Xu, S. Asahina, K. A. Cychoz, K. V. Agrawal, Y. A. Wahedi, A. Bhan, S. A. Hashimi, O. Terasaki, M. Thommes and M. Tsapatsis, *Science*, 2012, **29**, 1684.
- (a) Y. Han, F.-S. Xiao, S. Wu, Y. Sun, X. Meng, D. Li, S. Lin, F. Deng and X. Ai, *J. Phys. Chem. B*, 2001, **105**, 7963; (b) C. Li, Y. Q. Wang, Y. Guo, X. Liu, Y. Guo, Z. Zhang, Y. Wang and G. Lu, *Chem. Mater.*, 2007, **19**, 173; (c) Z. Zhang, Y. Han, L. Zhu, R. W. Wang, Y. Yu, S. L. Qiu, D. Y. Zhao and F.-S. Xiao, *Angew. Chem., Int. Ed.*, 2001, **40**, 1258.
- (a) E. Nikolla, Y. Román-Leshkov, M. Moliner and M. E. Davis, *ACS Catal.*, 2011, **1**, 408; (b) Y. J. Pagan-Torres, T. Wang, J. M. R. Gallo, B. H. Shanks and J. A. Dumesic, *ACS Catal.*, 2012, **2**, 930; (c) V. Choudhary, A. B. Pinar, S. L. Sandler, D. G. Vlachos and R. F. Lobo, *ACS Catal.*, 2011, **1**, 1724; (d) L. Li, I. Koranyi, B. F. Sels and P. P. Pescarmona, *Green Chem.*, 2012, **14**, 1611.
- (a) D. Zhao, Q. Huo, J. Feng, B. F. Chmelka and G. D. Stucky, *J. Am. Chem. Soc.*, 1998, **120**, 6024; (b) L. Wang, X. Meng, B. Wang, W. Chi and F.-S. Xiao, *Chem. Commun.*, 2010, **46**, 5003.
- (a) R. Xu, W. Pang, J. Yu, Q. Huo and J. Chen, *Chemistry of Zeolite and Related Porous Materials*, Wiley, Singapore, 2007; (b) L. Wang, J. Zhang, S. Yang, Q. Sun, L. Zhu, Q. Wu, H. Zhang, X. Meng and F.-S. Xiao, *J. Mater. Chem. A*, 2013, **1**, 9422.
- Y. Jin, P. Wang, D. Yin, J. Liu, H. Qiu and N. Yu, *Microporous Mesoporous Mater.*, 2008, **111**, 569.
- (a) A. K. Santra and D. W. Goodman, *J. Phys.: Condens. Matter*, 2003, **15**, R31; (b) G. K. Wertheim and S. B. Diczienzo, *Phys. Rev. B: Condens. Matter Mater. Phys.*, 1988, **37**, 844.
- (a) P. Li, G. Liu, H. Wu, Y. Liu, J. Jiang and P. Wu, *J. Phys. Chem. C*, 2011, **115**, 3663; (b) N. K. Mal, V. Ramaswamy, S. Ganapathy and A. V. Ramaswamy, *Appl. Catal., A*, 1995, **125**, 233; (c) S.-Y. Chen, H.-D. Tsai, W.-T. Chuang, J.-J. Lee, C.-Y. Tang, C.-Y. Lin and S. Cheng, *J. Phys. Chem. C*, 2009, **113**, 15226.

- 14 (a) Y. Wang, F. Wang, Q. Song, Q. Xin, S. Xu and J. Xu, *J. Am. Chem. Soc.*, 2013, **135**, 1506; (b) N. C. Yang, D. D. H. Yang and C. B. Ross, *J. Am. Chem. Soc.*, 1959, **81**, 133.
- 15 (a) R. Sasikala, A. R. Shirole, V. Sudarsan, V. S. Kamble, C. Sudakar, R. Naik, R. Rao and S. R. Bharadwaj, *Appl. Catal., A*, 2010, **390**, 245; (b) M. Tamura, K. Shimizu and A. Satsuma, *Appl. Catal., A*, 2012, **433**, 135.
- 16 (a) D. Tilman, J. Hill and C. Lehman, *Science*, 2006, **314**, 1598; (b) U. Biermann, U. Bornscheuer, M. A. R. Meier, J. O. Metzger and H. J. Schafer, *Angew. Chem., Int. Ed.*, 2011, **50**, 3854; (c) M. Pagliaro, R. Ciriminna, H. Kimura, M. Rossi and C. D. Pina, *Angew. Chem., Int. Ed.*, 2007, **46**, 4434; (d) H. Michel, *Angew. Chem., Int. Ed.*, 2012, **51**, 2516; (e) S. Wang, K. H. Yin, Y. C. Zhang and H. C. Liu, *ACS Catal.*, 2013, **3**, 2112; (f) J. Zhang, X. Liu, M. Sun, X. Ma and Y. Han, *ACS Catal.*, 2012, **2**, 1698; (g) J. Zhang, X. Liu, M. N. Hedhili, Y. H. Zhu and Y. Han, *ChemCatChem*, 2011, **3**, 1294; (h) S. H. Chai, H. P. Wang, Y. Liang and B.-Q. Xu, *Green Chem.*, 2008, **10**, 1087.
- 17 (a) Y. Roman-Leshkov, M. Moliner, J. A. Labinger and M. E. Davis, *Angew. Chem., Int. Ed.*, 2010, **49**, 8954; (b) G. Vicente, J. A. Melero, G. Morales, M. Paniagua and E. Martin, *Green Chem.*, 2010, **12**, 899; (c) C. X. A. da Silva, V. L. C. Goncalves and C. J. A. Mota, *Green Chem.*, 2009, **11**, 38.
- 18 (a) P. Shah and V. Ramaswamy, *Microporous Mesoporous Mater.*, 2008, **114**, 270; (b) R. Ryoo, S. Jun, J. M. Rim and M. J. Kim, *Chem. Commun.*, 1997, 2225.
- 19 (a) G. Busca, *Chem. Rev.*, 2007, **107**, 5366; (b) W. E. Farneth and R. J. Gorte, *Chem. Rev.*, 1995, **95**, 615.
- 20 (a) Q. Guo, F. Fan, E. A. Pidko, W. N. P. van der Graaff, Z. Feng, C. Li and E. J. M. Hensen, *ChemSusChem*, 2013, **6**, 1352; (b) M. S. Holm, S. Saravanamurugan and E. Taarning, *Science*, 2010, **328**, 602.
- 21 (a) V. Choudhary, S. H. Mushrif, C. Ho, A. Anderko, V. Nikolakis, N. S. Marinkovic, A. I. Frenkel, S. I. Sandler and D. G. Vlachos, *J. Am. Chem. Soc.*, 2013, **135**, 3997; (b) B. Kamm, *Angew. Chem., Int. Ed.*, 2007, **46**, 5056.